Molecular Dynamics Simulation of Time-Resolved Fluorescence Anisotropy Decays from Labeled Polyelectrolyte Chains

Peter Košovan, Zuzana Limpouchová, and Karel Procházka*

Department of Physical and Macromolecular Chemistry and Laboratory of Specialty Polymers, School of Science, Charles University in Prague, Albertov 2030, 12840 Prague 2, Czech Republic

Received November 30, 2005; Revised Manuscript Received March 15, 2006

ABSTRACT: Molecular dynamics simulations aimed at better understanding of the relationship between reorientational dynamics of pendant fluorescent probes and time-resolved fluorescence anisotropy on one hand and the segmental dynamics and conformations of the main polyelectrolyte chain on the other hand were performed. The simulation results provide a basis for an interpretation of fluorescence anisotropy decay measurements which are used to monitor conformational changes. Such measurements are indirect and require independent additional information on the studied system for a reliable interpretation. Our simulation results show a relation between the experimentally available rotational correlation times and the conformational behavior of the polymer. The simulation results were compared with published experimental data on poly(methacrylic acid) and a good qualitative agreement was found. Some differences in absolute values can be attributed to differences between the simulated and experimental systems.

Introduction

The ultrafast time-resolved fluorescence anisotropy belongs to the most popular techniques used for studying flexibility, chain conformations, and conformational changes of fluorescently labeled polymers. The experimentally available fluorescence characteristics of a fluorophore attached to the chain report on the interaction of the probe with its immediate microenvironment which depends on the chain conformation. There exist numerous fluorescence anisotropy studies on various polymer systems.[1,2] Even though the incorporation of an extrinsic fluorophore, which chemically differs from the monomer unit, modifies the chain behavior, fluorescence spectroscopy with extrinsic probes is generally recognized as a reasonable tool for studying the conformational behavior of polymers. Because it is an indirect technique and fluorescence spectra, quantum yields, lifetimes, etc. are sensitive to a number of effects, any reliable interpretation of experimental data should always be based on a combination of fluorescence measurements with other experimental techniques or computer modeling. In this work, we offer a new independent basis for unambiguous interpretation of experimental fluorescence data on labeled polyelectrolyte systems. Furthermore, we use the simulation results for comparison with our older data on PMA[2] and for interpretation of the experimental data in the context of the new results.

The behavior of PMA in aqueous solutions has been a subject of numerous studies.[3−6] Systematic studies of PMA in aqueous solutions started in the early fifties of the last century with the paper by Katchalski.[3] The most important achievements were made by Strauss et al.,[4] Morawetz et al.,[5] and by Ghiggino et al.[6] It was recognized that the behavior of PMA differs from that of a number of other polyelectrolytes (PEs), e.g., from the behavior of very similar poly(acrylic acid), PAA. At that time, PMA was usually described as a polyelectrolyte similar to polysoaps. Ghiggino[6] was the first who proposed the "necklace of pearls model", specifically for PMA in 1985, more than 10 years before a similar Dobrynin[7] model became popular.

Dobrynin, Rubinstein, and Obukhov proposed the "necklace of pearls model" as a general scheme of the behavior of strong (quenched) polyelectrolytes in bad solvents. They predicted theoretically a cascade of transitions from a collapsed globular conformation through the pearl-necklaces with increasing number of pearls toward the expanded conformation as a result of increasing ionization of the polyelectrolyte chain. Since water is a bad solvent for the polymer backbone of most polyelectrolytes and the solubility is achieved only due to the presence of charged hydrophilic groups, this model became fully recognized. The behavior of weak (annealed) polyelectrolytes exhibits specific features. It was shown theoretically by Raphael and Joanny[8] and later supported by Monte Carlo simulations,[9] that the reversible collapse/expansion of weak polyelectrolytes in very bad solvents should occur as a sudden first order transition. Nevertheless, a gradual transition via the necklace of pearls was predicted in a fairly narrow region of marginal solvents close to Θ-conditions.[10] Poly(methacrylic acid) contains a strongly hydrophobic methyl group and a carboxylic group in each repeating unit. The uncharged nondissociated carboxylic group is fairly hydrophilic, and this is why PMA is water-soluble to a certain extent at low pH. Hence, water is a marginal solvent for nonionized PMA, and the pH-induced transition should be gradual. We believe that the Dobrynin model offers a suitable basis for studying dynamic properties of PMA in aqueous buffers.

A number of studies have been devoted to the conformational behavior of PEs.[9−11] In this paper, we use molecular dynamics (MD) for the simulation of the time-resolved fluorescence anisotropy decays from fluorescently tagged polyelectrolyte chains in aqueous media. We want to explore the relations between the conformational behavior of the PE and the experimentally observable fluorescence anisotropy decays. This should provide a basis for an unambiguous interpretation of fluorescence measurements and we use it for the interpretation of our older experimental data on PMA.

The paper is organized as follows: first we describe the methodology of the simulation and the polymer model. Next, we define the most important fluorescence characteristics and

* To whom correspondence should be addressed.

10.1021/ma052557a CCC: $33.50
Published on Web 04/08/2006

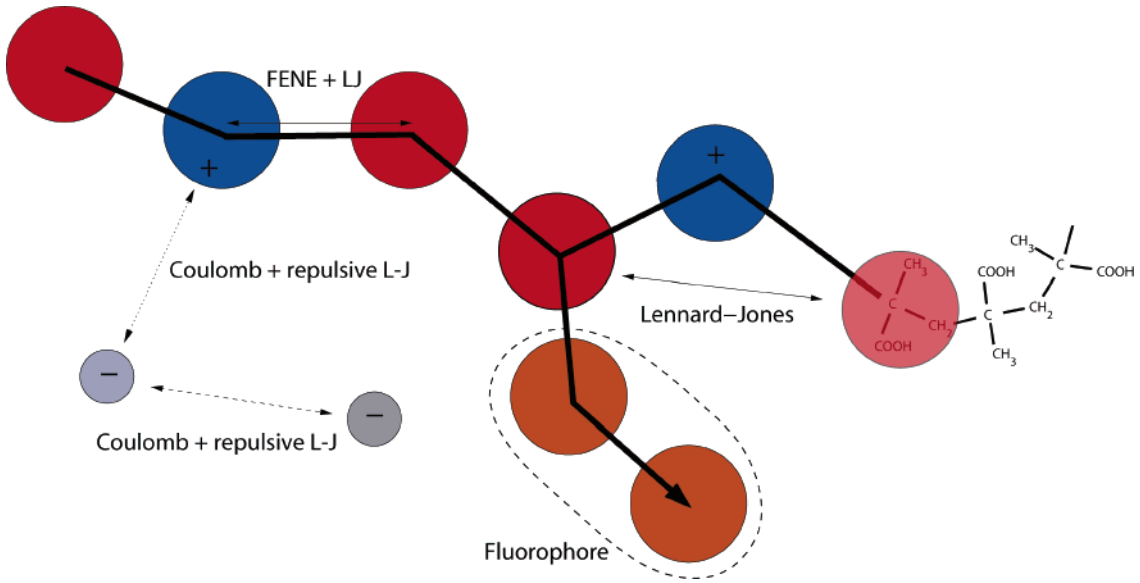

Figure 1. Schematic representation of the polymer model and the interactions. The fluorophore is attached to the side of the polymer backbone and the autocorrelation function of the vector indicated by the arrow is used for calculation of the fluorescence anisotropy.

briefly outline the method used for the calculation of time-resolved fluorescence anisotropy decays from computer simulations. We begin the discussion by commenting on the assumptions and simplifications used and discuss possible consequences. This is followed by the discussion of the conformational behavior and its relation to the time-resolved fluorescence depolarization. The last part is devoted to the comparison of the simulation results with our older experiments on poly(methacrylic acid) and interpretation of the experimental data in context of the simulations.

The Method

The Polymer Model. We are using a bead−spring freely jointed chain as our polymer model. The length of the backbone is 200 beads, each representing one monomer unit. The pendant fluorescent label is modeled by two beads attached to the side of the main backbone. The model is schematically depicted in Figure 1.

The van der Waals interactions between individual monomer units are modeled by the Lennard-Jones potential (LJ) with a finite cutoff and an appropriate shift

$$U_{LJ,hydrophob}(r_{ij}) = \begin{cases} 4\epsilon[(\sigma/r)^{12} - (\sigma/r)^6] - c(R_c) & \text{for } r \le R_c \\ 0 & \text{for } r > R_c \end{cases} \quad (1)$$

where $R_c = 2.5\sigma$ is the cutoff radius and $c(R_c) = (\sigma/R_c)^{12} - (\sigma/R_c)$.[6] The monomer units are usually hydrophobic and their mutual interaction results in an effective attraction when compared to the polymer−solvent interaction. The depth of the potential minimum, ϵ, controls the hydrophobicity of the polymer. The size of the monomer units is controlled by the σ parameter. The way how the values of the two parameters are set is described later.

In the case of small ions in the solution, there is no reason to expect an effective attraction typical for hydrophobic polymer molecules. Hence the excluded volume of small counterions is modeled by the purely repulsive part of the Lennard-Jones potential with an appropriate cutoff and shift

$$U_{LJ,hydrophil}(r) = \begin{cases} 4\epsilon[(\sigma/r)^{12} - (\sigma/r)^6] + \epsilon & \text{for } r < R_c = 2^{1/6}\sigma \\ 0 & \text{for } r > R_c \end{cases} \quad (2)$$

All parameters of eqs 1 and 2 are adjusted independently. For simplicity, we assume that the beads representing the fluorophore have the same interaction parameters as the monomer units of the polymer.

The chemical bonds along the polymer backbone are modeled by elastic forces described by the finite-extension nonlinear elastic (FENE) potential

$$U_{FENE}(r) = -(1/2)k_{FENE}R_{FENE}^2\ln\left(1 - \left(\frac{r}{R_{FENE}}\right)^2\right) \quad (3)$$

In this work we are using the values $k_{FENE} = 7.0\ kT/\sigma^2$ and $R_{FENE} = 2.0\ \sigma$, which, when combined with the Lennard-Jones potential, fixes the bond length roughly at 1.0 σ.

In an experiment, pH controls the degree of dissociation of a weak PE. In the simulation, we treat the degree of dissociation, α, as an adjustable parameter. The charges are placed uniformly along the chain and their position is fixed during the whole simulation. This is a good model for a quenched PE. For an annealed (weak) PE this is a simplification and its consequences will be discussed later.

The long-range nature of the electrostatic Coulomb potential does not allow for the use of a finite cutoff, as in the case of the LJ potential. The treatment of long-range forces requires special mathematical procedures for calculation. We use the Ewald summation calculated using the particle−particle particle−mesh algorithm, PPPM,[12] in the version presented by Petersen.[13]

The Simulation Technique. We are using molecular dynamics (MD) and our system is coupled to the Langevin thermostat, first described by Grest and Kremer.[14] The set of equations of motion reads

$$m\frac{d^2\vec{r}_i}{dt^2} = -\nabla\sum_{j\neq i}U(r_{ij}) + \vec{F}_i^{\,D} + \vec{F}_i^{\,R} \quad (4)$$

where $U(r)$ is the potential due to all types of interactions and $\vec{F}^D$ and $\vec{F}^R$ are the frictional and random forces, respectively. They are defined by the relations

$$\vec{F}_i^{\,D} = -m\Gamma\frac{d\vec{r}_i}{dt} \quad (5)$$

$$\langle\vec{F}_i^{\,R}(t)\cdot\vec{F}_i^{\,R}(t')\rangle = 6k_BTm\delta_{ij}\delta(t-t'); \quad \langle\vec{F}_i^{\,R}(t)\rangle = \vec{0} \quad (6)$$

where k_B is the Boltzmann constant, T is temperature and parameter Γ describes effective friction of the solvent, which is considered

as a continuous medium. In our simulations we are using $\Gamma = \tau^{-1}$ and the integration step of 0.0125 τ. The presence of the random forces implicitly accounts for collisions of monomer units with solvent molecules, which are not explicitly included in the simulation. The random force is generated from the Gaussian distribution and relation 6 ensures constant temperature during the simulation. The simulations were performed using the *ESPResSo* software package provided kindly by Limbach and Holm.[15]

Time and Length Scales in the Simulation. In simulations we use the monomer size, σ in eq 1, as the unit of length, monomer mass, m, as the unit of mass and kT ($T = 298$ K) as the unit of energy. To compare the simulation and the experiment, a unique relation between the units used in the simulation and those used by experimentalists is necessary. The experimental system of interest is PMA in aqueous solution. Hence we assume the size of one monomer unit (σ in eq 1) to be that of one ethylene group of PMA (2.49 Å). To fix the length scale we use the Bjerrum length, λ_B, defined as

$$\lambda_B = \frac{e^2}{4\pi\epsilon_0\epsilon_r k_B T} \tag{7}$$

We set the Bjerrum length to $\lambda_B = 2.85\sigma$, which corresponds to aqueous solutions at ambient temperature $T = 298$ K ($\lambda_B = 7.1$ Å). The size of the counterions (σ in eq 2) is assumed to be the same as that of the monomer unit. This size corresponds approximately to that of small ions (such as Na^+ or K^+) together with their first solvation shell.

The time scale is set by using the standard Lennard-Jones unit of time.[16]

$$t^* = \sigma\sqrt{m/kT} \tag{8}$$

For PMA monomer unit at ambient temperature we get $t^* \approx 1.5$ ns. The estimate of the size of the monomer unit is rather rough and so is also the estimated value of t^*. However, it makes it possible to compare the simulation data with experiment, at least at a semiquantitative level.

Time-Resolved Fluorescence Anisotropy. The time-resolved fluorescence anisotropy, $r(t)$, is defined as

$$r(t) = \frac{I_{||} - I_{\perp}}{I_{||} + 2I_{\perp}} = \frac{2}{5}\langle P_2\{\vec{\mu}_A(0)\cdot\vec{\mu}_E(t)\}\rangle \tag{9}$$

where $I_{||}$ and $I_{\perp}$ are the intensities of fluorescence polarized parallel and perpendicular to the plane of polarization of the exciting radiation pulse, respectively.[17] The right-hand side of eq 9 reflects the fact that $r(t)$ is given as an autocorrelation function of the absorption dipole moment of the fluorophore at time zero, $\vec{\mu}_A(t = 0)$, and its emission dipole moment at time t, $\vec{\mu}_E(t)$.[18] Here $P_2(x) = (1/2)(3x^2 - 1)$ is the second-order Legendre polynomial and the angular brackets denote ensemble average. The fluorophore is modeled by two beads attached to the polymer backbone as a pendant tag as shown in Figure 1. For the calculation of fluorescence anisotropy, we use the autocorrelation function of the vector pointing from one of the fluorophore-forming beads to the other, as indicated in Figure 1. For simplicity, we assume that the absorption and emission dipole moments are parallel. We also assume that the rotational diffusion is the only source of fluorescence depolarization and we neglect energy transfer and other processes that may occur in real systems.

Using the rotational diffusion model[19] it is possible to show that the time-resolved fluorescence anisotropy decay, $r(t)$, for a simple small and rigid fluorophore immersed in an isotropic solvent, can be expressed by the sum of up to five exponential functions, depending on the symmetry of the fluorophore

$$r(t) = \sum_{i=1}^{5} A_i \exp(-t/\tau_i) \tag{10}$$

where A_i and τ_i are individual preexponential factors and rotational correlation times, respectively. It is convenient to define the mean depolarization time, which reflects the overall rate of fluorescence depolarization

$$\tau_{mean} = \frac{\sum_i A_i\tau_i}{\sum_i A_i} = \int_0^\infty r(t)dt \tag{11}$$

In the case of a pendant fluorophore attached covalently to a flexible polymer chain, the situation is more complex. The rotation proceeds mainly around the bond connecting the fluorophore to the polymer backbone and it is strongly affected (hindered) by the instantaneous chain conformation. In a macroscopic sample the experimentally measured fluorescence depolarization reflects the average chain conformation.

Our study has shown that in comparison with simulation runs which are long enough for obtaining reasonably accurate static characteristics of the overall polymer conformations (such as the radius of gyration), considerably longer simulation runs are necessary to obtain statistically reliable fluorescence anisotropy decays. To obtain error estimates of the correlation times, we divide the whole simulation run into 10 equal sub-runs and calculate $r(t)$ and the corresponding correlation times for each of them. Then we calculate the standard deviation from the 10 obtained correlation times and use it as the error estimate. The overall anisotropy decay, $r(t)$, and the mean correlation time, τ_{mean}, are calculated from the whole simulation run which is set to be long enough to yield τ_{mean} with statistical error below 10%. Typically this is achieved within ca. $(5-8) \times 10^5 t^*$ which in real units means times around 1 ms, and the simulation requires about a week of CPU time on a 2 GHZ CPU.

Results and Discussion

General Remarks. The purpose of our study is to yield better insight into the complex relationship between average chain conformations and the segmental dynamics of the polyelectrolyte chain, on one hand, and the dynamics of a pendant fluorophore and experimentally observable ensemble average fluorescence depolarization response on the other hand. Before we start a systematic discussion of the simulation results, basic assumptions and simplifications used in our simulations have to be addressed.

(i) Although the study concerns general fluorescence behavior of tagged polyelectrolytes, we also want to compare the results of the simulations with experimental results for one specific system; i.e., we want to emulate our older experimental data on tagged PMA on a semiquantitative level. Contemporary MD methods do not offer any appropriate treatment of the reversible dynamic nature of dissociation of carboxylic groups (typical for annealed polyelectrolyte systems, such as PMA). Therefore, we use the degree of dissociation, α, as an adjustable parameter. We assume a uniform distribution of fixed charges along the polymer backbone and convert the pH effect to the α scale using the experimentally determined dependence of pK_a of PMA on pH.[20] Because the dissociation tendency of a particular $-$COOH group decreases after the dissociation of any other group in its vicinity, the charge distribution on an annealed PE is expected to be random, but fairly uniform. This assumption has also been supported by MC simulations of Uyaver and Seidel.[9] In the case of weak low molar mass acids, we could estimate the time scale on which the dissociation events occur using the estimates of dissociation rate constants from Brønsted relations.[21] For carboxylic acids, $k \approx 10^5$ s^{-1}, i.e., each individual COOH group dissociates once in about 10^{-5} s. This occurs at times much

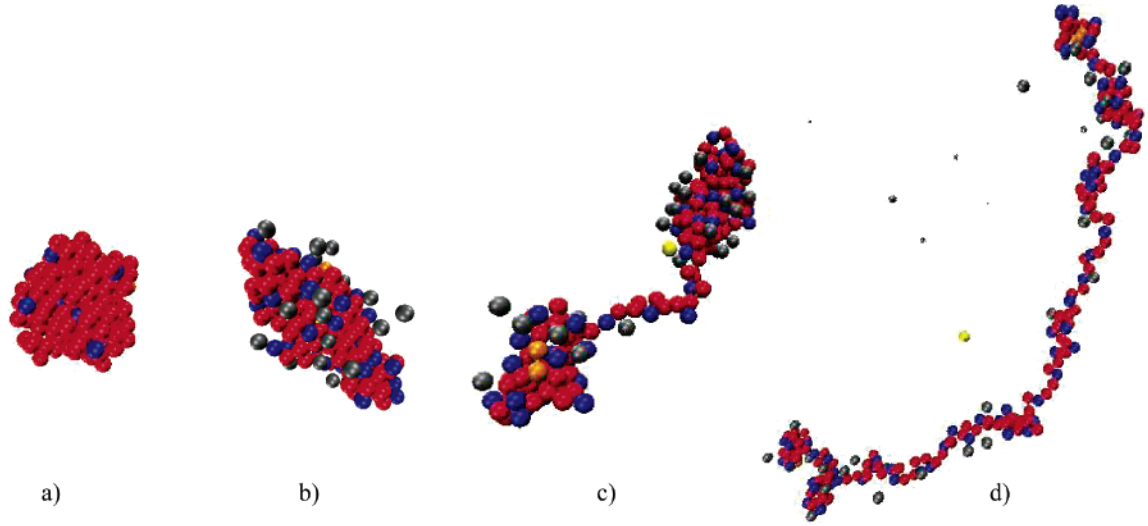

Figure 2. Variation of the conformation as a function of the degree of dissociation (α). Simulation snapshots of the polymer with $\epsilon = 1.3$, for $\alpha = 0.06$ (a), $\alpha = 0.20$ (b), $\alpha = 0.25$ (c), and $\alpha = 0.33$ (d). Key: red, uncharged monomer units; blue, charged monomer units; gray, counterions; orange, pendant fluorophore; yellow, center of mass of the chain. The snapshots differ in magnification; the real sizes of the monomer units are the same in all cases.

longer than the rotational correlation times obtained by experiment or simulation ($10^{-9}-10^{-8}$ s). Although other processes may occur in annealed polymer systems, e.g., the proton migration along the chain, the fast dynamic processes, such as the reorientation of pendant groups on the nanosecond scale, should not be affected by changing dissociation and should proceed quite similarly in annealed and quenched polyelectrolyte systems.

(ii) We study general behavior of polyelectrolytes in a broad range of conditions, the hydrophobicity of the polymer (ϵ in eq 2) has been used as an adjustable variable and we have performed a parametric study for $\epsilon = 1.0-2.0$. The range of ϵ reflects the fact that we are interested in fairly hydrophobic polymers. Further on we compare the simulation results to experimental data on PMA, which is presumably less hydrophobic than the model used. It is discussed in detail in the section where the comparison is made.

(iii) We are simulating a polymer in an implicit solvent, neglecting that in reality the solvent molecules affect the behavior of polymer chain. Perhaps the only correct way how to investigate the bias is to compare the results with simulations in an explicit solvent. Unfortunately, it is not computationally feasible for systems as large as ours. One might argue that at the time scales of 0.01 ns (ca our integration step), the collisions with solvent molecules are effectively uncorrelated and hence Markovian friction from the thermostat should be enough. However, the introduction of an implicit solvent may have a more profound effect. Certain attempts to explore it were made by Chang and Yethiraj.[22,23] They studied the collapse dynamics of neutral polymers and a range of concentrations of relatively short PEs ($N = 16$) in both an explicit solvent and an implicit solvent. Although they have studied processes that differ from those studied in this work, the message from their work is that the rearrangements of conformations in an explicit solvent are smoother than those in an implicit one and the dynamical behavior can be qualitatively different. According to their results, polymers in implicit solvents tend to be trapped in local energetic minima and the rearrangement of conformation into energetically more favorable state proceeds in a stepwise manner. Unlike Chang and Yethiraj, we are not interested in relaxation dynamics of collapsing polymer chain approaching equilibrium but in fluctuating equilibrium conformations. The lack of an explicit solvent can affect our simulations, but with simulation runs about 5 orders of magnitude larger than those used by Chang and Yethiraj, we sample a large number of fluctuations in conformation, which are hence properly statistically weighed (provided that our system is ergodic). Thus, we do believe that the use of implicit solvent does not distort the decisive qualitative relation between the conformational behavior and the time-resolved fluorescence anisotropy decay.

(iv) The simulations are very time-consuming, and CPU time demands increase steeply not only with the length of the chain but also even more with the number of charges. Hence, the simulated polyelectrolyte chains had to be shorter than those studied experimentally (monodisperse chains with M ca. 18000 compared to slightly polydisperse chains with M_w 27000 in the experiment). Thus, we should expect faster segmental dynamics from the simulation than from the experiments.

(v) The last issue to be mentioned is the flexibility of the chain. We are using the freely jointed chain, which results in segmental dynamics being faster than in real systems where bond angles are restricted and the rotation around the bonds is hindered.

The Conformational Behavior. We start with a brief summary of decisive features of the conformational behavior of simulated chains. Figure 2 shows four simulation snapshots presenting typical conformations of a polyelectrolyte chain with $\epsilon = 1.3$ at different dissociation degrees $\alpha = 0.06$ (a), 0.20 (b), 0.25 (c), and 0.33 (d). At a low degree of dissociation ($\alpha = 0.06$) the conformation is a compact (hypercoiled) globule (Figure 2a) and the polymer behaves effectively as in a bad solvent. With an increase in dissociation, the number of charged groups on the chain increases, and their mutual repulsion gains more significance, resulting in the chain expansion. At $\alpha = 0.20$ (Figure 2b), the conformation is still compact but it loses the spherical symmetry and resembles a prolate ellipsoid. The simulation movie reveals significant fluctuations in shape (available upon request). The ellipsoidal deformation was predicted by Khokhlov[24] several years before the Dobrynin paper was published. It was also pointed out by Khokhlov[25] that the expansion is a result of the complex behavior of the system containing both the polyelectrolyte chains and small ions. A further increase in the degree of dissociation results in the formation of the necklace of pearls conformation (Figure 2c

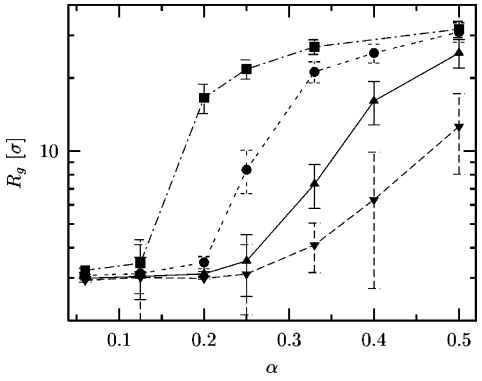

Figure 3. Radii of gyration, R_g, as functions of the degree of dissociation (α) for polymers of various hydrophobicities: $\epsilon = 1.0$ (■), $\epsilon = 1.3$ (●), $\epsilon = 1.6$ (▲), and $\epsilon = 2.0$ (▼).

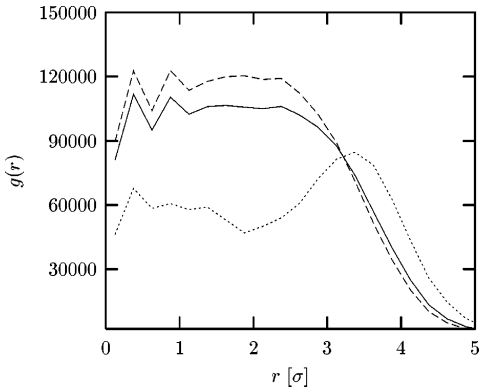

Figure 4. Angularly averaged distribution of segments around the center of mass of the polymer for the degree of dissociation $\alpha = 0.20$ and $\epsilon = 1.6$. Key: solid line, all types of segments; dashed line, uncharged segments; dotted line, charged segments.

for $\alpha = 0.25$). The structure is very dynamic and sometimes it is described as the "behavior of a frustrated polymer". The overall shape of the chain and the number and size of the "pearls" change many times during the simulation run. Starting at $\alpha = 0.33$ (Figure 2d), the conformations are stretched and slightly bent, forming a sausagelike shape.

Figure 3 shows radii of gyration, R_g, as functions of the dissociation degree, α, for a series of polymers differing in hydrophobicity, ϵ. The radius of gyration increases with α. In a marginal solvent with $\epsilon = 1.0$, the sigmoidal increase occurs between $\alpha = 0.125$ and 0.2, while in a really bad solvent with $\epsilon = 2.0$, the onset of the change is shifted toward fairly high dissociation degrees above $\alpha = 0.3$. The increasing part of the curve corresponds generally to the pearl-necklace structure. In this region, the simulation errors increase considerably due to the dynamic "frustration behavior", i.e., due to large fluctuations in chain conformations. It is also important to note that the shape of the curves is qualitatively similar for all ϵ values, but the changes occur at different α.

Figure 4 shows the angularly averaged distribution of segments around the center of gravity for the chain with $\alpha = 0.20$ and $\epsilon = 1.6$, which corresponds to a fluctuating but still fairly compact prolate ellipsoid. The full line depicts the distribution of all segments, while the dashed and dotted ones refer to neutral and electrically charged beads, respectively. The dotted curve with a maximum at around 3.5 σ suggests that the charged beads are localized preferentially at the surface of compact structures. The same effect can be observed in other globular systems, although it disappears at the globule−necklace-of-pearls transition, presumably due to the large fluctuations described above. The dissociation of annealed

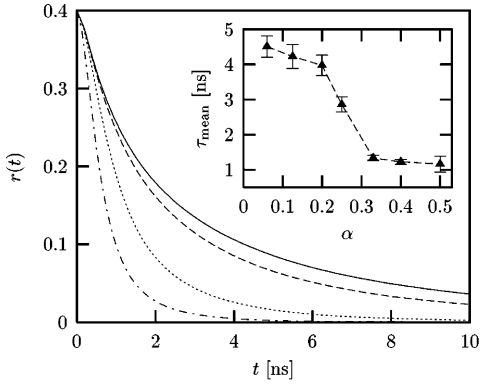

Figure 5. Simulated anisotropy decays for a polymer with $\epsilon = 1.3$ for selected degrees of dissociation, α, in the range of the conformational transition. Key: full line, $\alpha = 0.20$; dashed line, $\alpha = 0.25$; dotted line, $\alpha = 0.33$; dash−dot line, $\alpha = 0.4$. Insert: the mean correlation times as a function of α for the same polymer.

polyelectrolytes is promoted at the periphery of compact globules due to the exposure to the aqueous medium. In our simulation the unlimited flexibility of model chains allows an enhanced concentration of charged groups at the surface of compact polymeric domains. Although the simulation was done for a quenched polyelectrolyte, we observe that the overall structure is reproduced. If it were not so and the charged groups were evenly distributed in the whole volume of the globule, the electrostatic repulsion between the charges would swell the chain in moderately bad solvents and thus significantly change the conformational behavior. Such swelling might easily occur in the case of more geometrically constrained quenched PE, however, due to mobility of charges, it is not expected to occur in the case of an annealed one. We cannot preclude that the simplification used does not shift the transition to worse thermodynamic conditions, but we may conclude that the unlimited flexibility makes up for the fixation of charges and hence the model is applicable for annealed PEs.

Time-Resolved Fluorescence Anisotropy Decays. We have studied both the chains tagged by a pendant fluorophore and by a fluorophore incorporated as a comonomer in the polymer chain. Since the results did not significantly differ and our experimental data concern PMA with pendant dansyl groups, we present computer data for the former case only. Typical fluorescence anisotropy decay curves for system with $\epsilon = 1.3$ are reproduced in Figure 5. Since we assume the reorientation motion of the fluorophore as the only source of depolarization, the effective rotation correlation time corresponds to the measured depolarization time. It is evident that the decreasing degree of ionization slows down the motion of the pendant fluorophore and the fluorescence depolarization. The curves are not single-exponential and can be fitted reasonably well by double-exponential functions. However, we use the mean depolarization time, (see eq 11), in the discussion of the trends observed in the simulated behavior. The real depolarization motion of pendant tags is a fairly complex process. In reality, it is a combination of different types of motion, which cannot be discerned in a coarse-grained model. Therefore, any reasonable and straightforward discussion can be based on the mean depolarization time only.

Changes in the mean depolarization time with solvent quality and the degree of dissociation are summarized in Figure 6. For systems in moderately bad solvents ($\epsilon = 1.0$ and 1.3), a considerable expansion of the chain occurs in the studied range of dissociation degrees, together with a pronounced sigmoidal decrease in the mean depolarization time, τ_{mean}. With decreasing

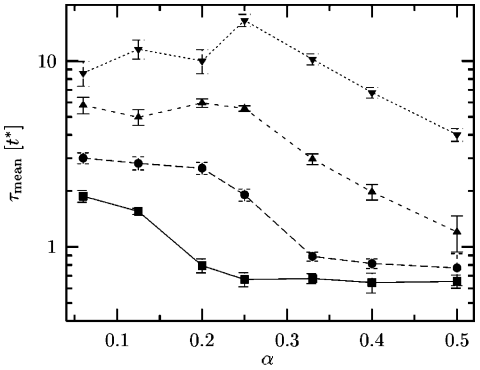

Figure 6. Mean rotational times as a function of the degree of dissociation (α) for polymers of various hydrophobicities: $\epsilon = 1.0$ (■), $\epsilon = 1.3$ (●),$\epsilon = 1.6$ (▲), $\epsilon = 2.0$ (▼).

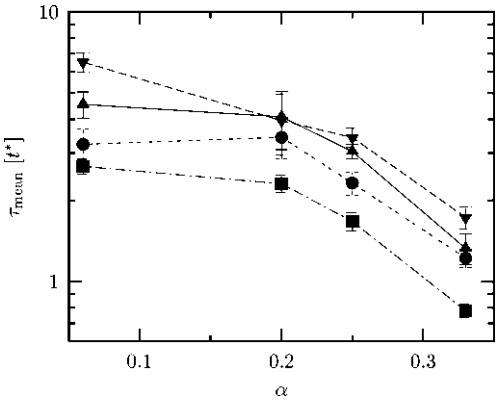

Figure 7. Mean rotational times as a function of the degree of dissociation (a) for a polymer of $\epsilon = 1.3$ labeled with fluorophores of various hydrophobicities: $\epsilon = 1.3$ (■), $\epsilon = 1.6$ (●), $\epsilon = 2.0$ (▲), and $\epsilon = 2.3$ (▼).

solvent quality, the sigmoidal decrease in the mean depolarization time and the increase in R_g shift toward higher degrees of dissociation. In very bad solvents, only the onsets of changes in the characteristics were observed. It is important to notice that, for a given ϵ, both the changes in the correlation times and the conformational changes occur at the same value of α.

For high values of α, i.e., in the region of highly expanded conformations, the fast depolarization times converge to the same value for all systems, independent of ϵ. This suggests that the depolarization is due to an almost unhindered motion of pendant fluorophore exposed to the surrounding solvent.

For simplicity, in most simulations we have used the same parameters for the fluorophore as those for monomer units of the polymer chain. In reality, the fluorophore is more hydrophobic than the polymer, which can affect the experimental rotational correlation times. We have performed a set of simulations verifying that the simulated rotational correlation time grows with the hydrophobicity of the fluorophore. Its dependence on the fluorophore hydrophobicity is depicted in Figure 7. We have found that only the absolute values of the rotation correlation time change, but all decisive trends remain qualitatively the same, which justifies the qualitative comparison based on the model with fluorophores with the same parameters as the monomer units.

Comparison of the Simulated and Experimental Data. In an earlier experimental paper we have studied the behavior of poly(methacrylic acidic) tagged by pendant dansyl groups in dilute aqueous solutions as a function of pH.[2] Several tagged PMA samples differing in the length and degree of tagging were synthesized and the time-resolved fluorescence decays and time-resolved anisotropies were measured. Both types of decays were essentially double-exponential and their characteristic parameters (marked differently in the original paper) were found to depend considerably on pH and ionic strength. In the region close to pH 5, we have observed abrupt changes both in fluorescence lifetimes, τ_F, and in rotational correlation times, τ_C. However, the decrease in fluorescence lifetimes with increasing pH started appreciably later and finished slightly earlier; i.e., the drop was faster as compared with changes in rotational correlation times. Although the observed increase in fluorescence lifetimes was steep, it was far from being discontinuous. Moreover, the dependence of depolarization times, τ_C, went through a maximum close to pH 4.

At that time, a very vivid discussion concerning the PMA supercoiling took place. It was focused mainly on the question whether the conformational change with pH is a cooperative (i.e., steep or almost discontinuous) or progressive (continuous) process. We have interpreted our experimental data in the following way: the fluorescence lifetimes report on the interaction of the fluorophore with the microenvironment. When pH decreases, the stretched chains start to collapse and supercoil. As the fluorophore is more hydrophobic than the monomer, its presence induces the reorganization of monomer units and solvent molecules first in its immediate vicinity. Close to pH 6, the microenvironment of the fluorophore changes considerably but independently of the conformational behavior of the rest of the chain. The measured fluorescence lifetimes reflect only the microenvironment and they change steeply. The fact that the depolarization times change more slowly may be accounted for as follows: at high pH, the chain is stretched and the rotation of the fluorophore around the spacer single bonds is almost unhindered. The corresponding rotation correlation time is short. The observed continuous increase in τ_C with decreasing pH suggests that the probe is trapped in collapsing and simultaneously growing domains. Hence the fact that the rate of fluorescence depolarization slows down continuously and the maximum is attained at lower pH (as compared with τ_F) does not seem to support the concept of a cooperative transition but it can be considered as a support for the hypothesis of continuous conformational changes. Despite a number of later experimental and theoretical studies,[9−11,20,26] the above question has not been unambiguously solved until now. As mentioned above, theoretical studies by Raphael and Joanny[8] and recent Monte Carlo simulations by Uyaver and Seidel[9,10] seem to indicate that a sudden sharp transition from a very compact globule to an almost fully stretched chain conformation occurs in very bad solvents, while in solvents of medium quality a gradual transition via the "necklace of pearls" arrangements takes place. As concerns PMA, water is a bad but certainly not too bad solvent because the nondissociated, i.e., uncharged, COOH is a hydrophilic group, and almost neutral PMA is still partly soluble at low pH.

Literature reports the Θ-temperature for PMA dissolved in 0.05 M NaCl, which roughly corresponds to the system studied by the experiment, to be 68 °C.[27] Raphael and Joanny[8] define the rescaled distance from the Θ-point

$$\tau = (\theta - T)/\theta \tag{12}$$

They have shown that the conformational transition should be smooth for $\tau < N^{-1/5}\, u^{-3/5}$, where N is the number of monomer units per chain and $u = \lambda_B/a$, where a is the monomer size (corresponding to σ in our work). Using $u = 2.85$ and $N = 313$ for the system studied by the experiment, we get $\tau = 0.14 < \tau_c = 0.17$, where τ_c is the critical value $\tau_c = N^{-1/5}\, u^{-3/5}$. Hence,

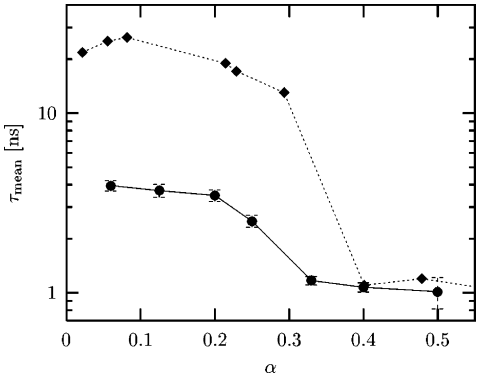

Figure 8. Comparison of the simulation and the experiment: polymer with $\epsilon = 1.3$(●); experimental data on PMA (◆).

PMA should be in the region of smooth conformational transition, and the use of a model where both α and conformations vary continuously is justified. Yet it should be kept in mind that the comparison is tricky, because the Θ-temperature used by Raphael and Joannhy[8] refers to a neutral chain having the same interaction parameters as the weak polyelectrolyte. This requirement is unattainable in experiment, so one has to choose a compromise, which hopefully is not far from the theoretical Θ-temperature. In our study, we have chosen the value that fit best this requirement.

Grest and Murat[28] have determined the Θ-temperature for a neutral polymer described by the Lennard-Jones potential $T_\Theta^* = 3.0 \pm 0.2$ for $\epsilon = 1.0$, which corresponds to $\epsilon \approx 0.3kT$ in our system of reduced units. The use of our set of reduced units allows us to separate the effect of polymer hydrophobicity from other effects. This is desirable because the hydrophobicity, ϵ, is the only unknown variable whereas all others, such as λ_B or T can be taken directly from experiment (see also Micka et al.[29] for discussion of this issue). However, when comparing the simulated systems to the critical values presented in the previous paragraph, it is convenient to use the set of reduced units of Grest and Murat,[28] i.e., to set ϵ values for all the systems to 1.0 and rescale the reduced temperatures appropriately, so as to keep the ratio ϵ/T^* constant. Then the distances from the Θ-point, used in our work, are $\tau = 0.66-0.83$. By using a poorer solvent, we compensate for technical limitations concerning the restricted chain length and the number of charges present in the simulation. Ideally, we should have simulated longer chains with $\tau \approx 0.14$. This would have resulted in a more expanded conformation at the same value of α. The real system also contains salt ions, which effectively weaken the electrostatic repulsion among the dissociated monomer units by screening the charges, resulting in a more compact conformation. Hence, the use of shorter chains further from the Θ-point partly compensates for the lack of the salt, resulting in a model which is computationally feasible.

To compare simulation results with the experiment, we had to put both sets of data on the same scale. For the time scale, we use the reduced time unit $t^* \approx 1.5$ ns. For the conversion of pH-dependent experimental data to the α scale, we use the dependence of pK_a of PMA on pH published in the literature.[20] The comparison of the simulated depolarization times for a system with $\epsilon = 1.3$ with experimental data is shown in Figure 8. Although both the model and experimental systems and conditions slightly differ, the agreement is fairly nice as concerns the shape of the curves. Hence, the molecular dynamics simulation reproduces all decisive trends fairly well, which can also be considered as evidence of the proper choice of the used simulation technique for studying the above problem.

The differences in absolute values, i.e., shorter times obtained by the simulation, arise for several reasons. In the first place, the simulation is primarily a parametric study of the general behavior of polyelectrolytes (for PMA, we have simply chosen a reasonable value of ϵ, which best fits the experimental data) and the value of t^* is a rather crude estimate. Second, the simulated chains are coarse grained, shorter and more flexible than the real ones. As already mentioned, it results in shorter correlation times for both collapsed and stretched conformations.

Conclusions

The presented molecular dynamics simulations help to understand the relationship between the conformational behavior of polyelectrolytes and the time-resolved fluorescence depolarization from pendant tags. The obtained information provides a basis for unambiguous interpretation of results of fluorescence measurements and shows a relation between the rotational correlation times and the conformational behavior of the polymer.

The simulation results are in a reasonable semiquantitative agreement with experimental data on poly(methacrylic acid). Some differences in absolute values can be attributed to the differences between the simulated and experimental systems.

The state of art in MD simulations and technical limitations do not allow us to simulate exactly the same system that we studied experimentally. The performed simulations preserve the key qualitative features of real systems, however, we do not claim more than a semiquantitative agreement. Some simplifications used induce faster segmental dynamics of the chain as compared with real one, while the effect of the others can be only hardly quantified.

Even though it will not possible to avoid technical limitation in near future, some conceptual difficulties can be overcome. It is highly desirable to develop a proper parametrization of the model, e.g., using a systematically derived coarse-grained potential, and to devise a method for simulating annealed polyelectrolytes using MD. These are challenging tasks which should be addressed in future.

Acknowledgment. K.P. and Z.L. thank the Grant Agency of the Czech Republic (Grant No. 203/03/0262, and Grant No. 203/04/0490) and the Marie Curie Research and Training Network (Grant No. 505 027, POLYAMPHI) for the support. P.K. would like to thank the Grant Agency of the Czech Republic (Grant No. 203/04/P117) for the financial support. We would like to thank H. J. Limbach and C. Holm for kindly providing the *ESPResSo* software. We also would like to thank our colleagues Filip Uhlík and Karel Jelínek for help with programming and fruitful discussions.

References and Notes

(1) (a) Anrufieva, E. V.; Gotlib, Y. Y. *Adv. Polym. Sci.* **1981**, *40*, 1. (b) Tan, K. L.; Treolar, F. E. *Chem. Phys. Lett.* **1980**, *73*, 239. (c) Fleming, G. R. *Chemical Applications of Ultrafast Fluorescence Spectroscopy*, Oxford University Press: New York, 1986. (d) Miguel, M. D. *Adv. Colloid Interface Sci.* **2001**, *89*, 1. (e) Winnik, M. A. *Photophysical and Photochemical Tools in Polymer Science*; Winnik, M. A., Ed.; NATO ASI Series C, Vol. 182; Riedel: Dordrecht, The Netherlands, 1986. (f) Ediger, M. D. *Annu. Rev. Phys. Chem.* **1991**, *42*, 225. (h) Chee, C. K.; Rimmer, S.; Soutar, I.; Swanson, L. *Polymer* **1997**, *38*, 483. (i) Soutar, I. *Polym. Int.* **1991**, *26*, 35. (j) Winnik, F. M.; Regismond, S. T. A. *Colloids Surf. A—Physicochem. Eng. Asp.* **1996**, *118*, 1. (k) Ghiggino, K. P.; Roberts, A. J.; Phillips, D. *Adv. Polym. Sci.* **1981**, *40*, 69. (l) Johnson, B. S.; Ediger, M. D.; Kitano, T.; Ito, K. *Macromolecules* **1992**, *25*, 873. (m) Soutar, I.; Swanson, L. *Macromol. Symp.* **1995**, *90*, 267. (n) Procházka, K.; Medhage, B.; Mukhtar, E.; Almgren, M.; Svoboda, P.; Trněná, J.; Bednář, B. *Polymer* **1993**, *34*, 103. (o) Chee, C. K.; Ghiggino, K. P.; Smith, T.

A.; Rimmer, S.; Soutar, I.; Swanson, L. *Polymer* **2001**, *42*, 2235. (p) Soutar, I.; Swanson, L. *ACS Symp. Ser.* **1995**, *568*, 388. (q) Ebdon, J. R.; Soutar, I.; Brown, P.; Lane, A. R.; McCabe, A. J.; Swanson, L. *J. Polym. Sci., Part B: Polym. Phys.* **1999**, *37*, 2127.
(2) Bednář, B.; Trněná, J.; Svoboda, P.; Vajda, Š.; Fidler, V.; Procházka, K. *Macromolecules* **1991**, *24*, 2054.
(3) Katchalski, A. *J. Polym. Sci.* **1951**, *7*, 393.
(4) (a) Strauss, U.; P.; Vesnaver, G. *J. Phys. Chem.* **1975**, *79*, 1558. (b) Strauss, U.; P.; Schlesinger, M. S. *J. Phys. Chem.* **1978**, *82*, 1627.
(5) Wang, Y.; Morawetz, H. *Macromolecules* **1986**, *19*, 1925.
(6) Ghiggino, K.; P.; Tan, K. L. In *Polymer Photophysics*; Phillips, D., Ed., Chapman and Hall: London, 1985.
(7) Dobrynin, A.; V.; Rubinstein, M.; Obukhov, S. P. *Macromolecules* **1996**, *29*, 2974.
(8) Raphael, E.; Joanny, J.-F. *Europhys. Lett.* **1990**, *13*, 623.
(9) Uyaver, S.; Seidel, C. *Europhys. Lett.* **2003**, *64*, 536.
(10) Uyaver, S.; Seidel, C. *J. Phys. Chem. B* **2004**, *108*, 18804.
(11) (a) Limbach, H. J.; Holm, C.; Kremer, K. *Macromol. Symp.* **2004**, *211*, 43. (b) Limbach, H. J.; Holm, C. *J. Phys. Chem. B* **2003**, *32*, 2041.
(12) Darden, T.; York, D.; Pedersen, L. *J. Chem. Phys.* **1993**, *98*, 10089.
(13) Petersen, H. G. *J. Chem. Phys.* **1995**, *103*, 3668.
(14) Grest, G. S.; Kremer, K. *Phys. Rev. A* **1986**, *33*, 3628.
(15) www.espresso.mpg.de.
(16) Stevens, M.; Kremer, K. *J. Chem. Phys.* **1995**, *103*, 1669.
(17) O'Connor, D. V.; Phillips, D. *Time-correlated single-photon counting*; Academic Press: London, 1984.
(18) Szabo, A. *J. Chem. Phys.* **1984**, *81*, 150.
(19) Belford, G. G.; Belford, R. L.; Weber, G. *Proc. Natl. Acad. Sci. U.S.A.* **1972**, *69*, 1932.
(20) Heitz, C.; Rawiso, M.; Francois, J. *Polymer* **1999**, *40*, 1637.
(21) Adamson, A. W. *A Textbook of Physical Chemistry*, 2nd ed.; Academic Press: New York, 1979.
(22) Chang, R.; Yethiraj, A. *J. Chem. Phys.* **2001**, *114*, 7688.
(23) Chang, R.; Yethiraj, A. *J. Chem. Phys.* **2003**, *118*, 6634.
(24) Khokhlov, A. R. *J. Phys. A* **1980**, *13*, 979.
(25) Khokhlov, A. R.; Nyrkova, I. A. *Macromolecules* **1992**, *25*, 1493.
(26) (a) Soutar, I.; Swanson, L. *Macromolecules* **1994**, *27*, 4304.
(27) Kanevskaya, Ye. A.; Zubov, P. I.; Ivanova, L. V.; Lipatov, Y. S. *Vysokomol. Soedin.* **1964**, *6*, 981; *Polym. Sci. USSR* **1964**, *6*, 1080.
(28) Micka, U.; Holm, C.; Kremer, K. *Langmuir* **1999**, *15*, 4033.
(29) Grest, G. S.; Murat, M. *Macromolecules* **1993**, *26*, 3108.

MA052557A